Received: 10 October 2018 | Revised: 20 January 2019 | Accepted: 20 January 2019

DOI: 10.1002/kin.21255

ARTICLE

WILEY

Ab initio thermal rate coefficients for $H + NH_3 \rightleftharpoons H_2 + NH_2$

Thanh Lam Nguyen | John F. Stanton

Quantum Theory Project, Departments of Chemistry and Physics, University of Florida, Gainesville, Florida

Correspondence
John F. Stanton, Quantum Theory Project, Departments of Chemistry and Physics, University of Florida, Gainesville, FL 32611.
Email: johnstanton@ufl.edu

Funding information
U.S. Department of Energy, Office of Basic Energy Sciences, Grant/Award Number: DE-FG02-07ER15884; U.S. Air Force Office of Scientific Research, Grant/Award Number: FA9550-16-1-0117; U.S. National Science Foundation, Grant/Award Number: CHE-1748821

Abstract

The reversible reaction $NH_3 + H \rightleftharpoons H_2 + NH_2$, which plays an important role in NH_3 fuel combustion, is studied with a theoretical approach that combines the high-accuracy extrapolated ab initio thermochemistry (HEAT) protocol with semiclassical transition state theory (SCTST). The calculated forward reaction is endothermic by 11.8 ± 1 kJ/mol, in nearly perfect agreement with the active thermochemical tables (ATcT) value of 11.5 ± 0.2 kJ/mol. Using this improved thermochemistry yields better rate constants, especially at low temperatures. Experimental rate constants available from 400 to 2000 K for the forward and reverse reaction pathways can be reproduced (within 20%) by the calculations from first principles.

KEYWORDS
HEAT, NH3, SCTST, VPT2

1 | INTRODUCTION

Carbon dioxide (CO_2) emissions into the atmosphere result in great part from combustion of fossil fuel, and this greenhouse gas is believed to be a potential source of global warming and a driver of climate change. In the context of clean combustion, hydrogen (H_2) fuel is considered as a nearly ideal and renewable energy source.[1–3] In contrast to fossil fuels, its combustion in air produces water vapor and small amounts of nitrogen oxides; it produces no carbon dioxide (CO_2) nor any compounds that will impact the ozone layer.[1–3] However, a mitigating consideration is that hydrogen fuel has a low-energy density, and therefore expensive to store and transport.[1–3]

Another simple and widely available compound that admits to clean combustion is ammonia (NH_3). In the thermal DeNO$_x$ process,[4–6] NH_3 is often supplied to transform NO_x species to N_2 and H_2O. Combustion of ammonia liberates water vapor, molecular nitrogen, and nitrogen oxides (NO_x)[7–10], all of which are environmentally innocuous. Given these favorable properties, it is not surprising that ammonia (NH_3) has been predicted to become a viable carbon-free energy source, especially in the transportation sector.[7–10]

We are currently interested in studying the mechanism, thermochemistry, and kinetics of fundamental reactions relevant to ammonia combustion. In a previous work,[11] we have reported thermal rate constants for the OH-oxidation of NH_3. In this work, we calculate the thermochemistry and the thermal rate constants for the similar $H + NH_3 \rightleftharpoons H_2 + NH_2$ reaction using the same theoretical approach as that taken previously.[11] The H-abstraction reaction $H + NH_3 \rightleftharpoons H_2 + NH_2$ has been fairly well studied both experimentally[12–18] and theoretically.[19–30] In addition, a nine-dimensional global potential energy surface of NH_4 and quantum dynamic calculations have been reported.[19–30] Therefore, a large amount of data is available to compare with our high-accuracy extrapolated ab initio thermochemistry (HEAT)/semiclassical transition state theory (SCTST) results.

2 | THEORETICAL METHODOLOGY

The same approaches that have been used successfully for the $OH + NH_3$ reaction[11] are reemployed here. Briefly, the high-level HEAT-456QP method—which can yield an accuracy of 1 kJ/mol—is used to compute thermochemistry and provide rovibrational parameters as well as anharmonic constants for the purpose of chemical kinetics. Except the CCSDTQP energy calculations that use MRCC program,[31] the other calculations are done using CFOUR quantum chemistry program.[32] The forward and reverse rate coefficients for the title reaction as displayed in Figure 1 can be

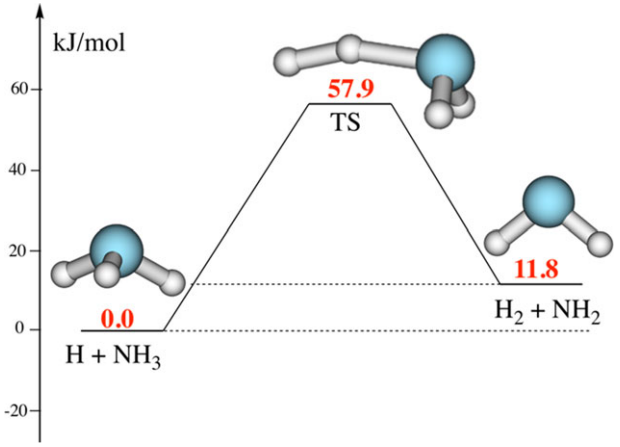

FIGURE 1 Schematic reaction energy profile for the H + NH_3 ⇌ H_2 + NH_2 reaction calculated using the HEAT-456QP method [Color figure can be viewed at wileyonlinelibrary.com]

computed at the high-pressure limit using Equations 1 and 2, respectively:

$$k(T)_{H+NH_3} = \frac{\sigma_1}{h}\left\{Q_e^{\neq}Q_{tr}^{\neq}\right\} \times \frac{\sum_{J=0}^{\infty}(2J+1)\int_{E=0}^{\infty}G_{rv}^{\neq}(E,J)\exp\left(-\frac{E}{k_BT}\right)dE}{Q_H^{re}Q_{NH_3}^{re}} \quad (1)$$

$$k(T)_{H_2+NH_2} = \frac{\sigma_2}{h}\left\{Q_e^{\neq}Q_{tr}^{\neq}\right\} \times \frac{\sum_{J=0}^{\infty}(2J+1)\int_{E=0}^{\infty}G_{rv}^{\neq}(E,J)\exp\left(-\frac{E}{k_BT}\right)dE}{Q_{H_2}^{re}Q_{NH_2}^{re}} \quad (2)$$

where k_B is Boltzmann's constant, h is Planck's constant, and σ_1 and σ_2 are the reaction path degeneracies, which are 3 and 4 for the forward and reverse reactions, respectively. Q_{tr} and Q_e are the translational and electronic partition functions for the transition state (TS). The electronic partition functions of the H atom, NH_2, and the TS for a doublet electronic state are equal to 2. Q_H^{re}, $Q_{H_2}^{re}$, $Q_{NH_2}^{re}$, and $Q_{NH_3}^{re}$ are the complete partition functions for the associated species. $G_{rv}^{\neq}(E,J)$ is the rovibrational cumulative reaction probability of transition state, which can be calculated by convolution of vibrational and rotational quantum states:

$$G_{rv}^{\neq}(E,J) = \int_0^E G_v^{\neq}(E_v)\,\rho_r^{\neq}(E-E_v)\,dE_v \quad (3)$$

where v and r stand for vibrational and rotational degrees of freedom, respectively. The SCTST code[33,34] of the MULTIWELL software package[35,36] was used to compute the sum of fully coupled vibrational states ($G_v^{\neq}(E_v)$) using a bin size of 1 cm^{-1} and a ceiling energy of 50,000 cm^{-1}. Assume that the TS can be approximated as a rigid-rotor symmetric top,[37] and the density of external rotational states ($\rho_r^{\neq}$) was counted directly using the following equation:

$$E_r = \overline{B}J(J+1) + \left(A-\overline{B}\right)K^2 \quad \text{with} \quad \overline{B} = \sqrt{B\cdot C} \quad \text{and} \quad -J \le K \le +J \quad (4)$$

Recently, we have studied fourth-order vibrational perturbation theory (VPT4) applied to the one-dimensional symmetric Eckart potential,[38] and we have found that some effects of higher order perturbation theory within the SCTST framework can heuristically be included by a rescaling of the barrier frequency used in the VPT2 treatment (Equation 5).[38] This approach, designated as "*SCTST/VPT2+*", seems to work well for the OH + NH_3 → H_2O + NH_2 reaction,[39] especially in the deep-tunneling regime. Note that this approach is available in the SCTST code of the MULTIWELL software package (keyword "VPT4A").

$$\left|\omega_F^{new}\right| = \left|\omega_F\right| \times \sqrt{1-\left(x_{FF}/\left|\omega_F\right|\right)^2} \quad (5)$$

In this work, we used both SCTST/VPT2 and SCTST/VPT2+ approaches to calculate thermal rate coefficients. However, the empirical adjustment defined by SCTST/VPT2+ lowers the barrier frequency ω_F by about 1.2%, resulting in a slight widening of the barrier. This small change reduces the calculated rate constants marginally for the temperature range of 300–2500 K (see below). Therefore, unless mentioned otherwise, SCTST/VPT2+ approach will be used for the following discussion.

3 | RESULTS AND DISCUSSION

3.1 | Thermochemistry

Table 1 shows a comparison of theory and experiment for spectroscopic parameters for NH_3, NH_2, and H_2, which are well established experimentally. As can be seen in Table 1, the CCSD(T) calculations are close to the experimental results apart from the (large amplitude) umbrella inversion motion of NH_3, but this agreement is still adequate for the purposes of determining zero point energies and densities of states needed for kinetic calculations. Table 2 shows the forward reaction pathway being endothermic by 11.8 ± 1.0 kJ/mol, which is in almost perfect agreement with the ATcT value of 11.5 ± 0.2 kJ/mol.[40–43] In addition, Table 2 also reveals individual contributions of various terms to a total activation energy. Inspection of Table 2 shows that the SCF method significantly overestimates the total barrier by nearly a factor of two. The CCSD(T) correction is the most important: it recovers most of the electron correlation, together with the SCF

TABLE 1 A comparison of theory with experiment for spectroscopic parameters of H_2, NH_2, and NH_3

Molecule	Parameter	ANO2/ANO1	aCVQZ/aCVTZ	Exptl.[a]
H_2 ($D_{\infty h}$, $X^1\Sigma_g$)	ω (cm^{-1})	4406	4400	4401.21
	X_{11} (cm^{-1})	–121.8763	–127.4246	–121.33
	B_e (cm^{-1})	60.7488	60.7631	60.853
	ν (cm^{-1})	4162	4145	4161.17
	H–H (Å)	0.7421	0.7420	0.74144
NH_2 (C_{2v}, X^2A_1)	ν_1 (cm^{-1})	1506	1498	1497.32
	ν_2 (cm^{-1})	3217	3225	3219.37
	ν_3 (cm^{-1})	3296	3305	3301.11
	A_e (cm^{-1})	23.3488	23.5724	23.72
	B_e (cm^{-1})	13.0250	12.9988	12.94
	C_e (cm^{-1})	8.3609	8.3785	8.16
	N–H (Å)	1.0256	1.0242	1.024
	∠HNH (degree)	102.7616	103.1014	103.4
NH_3 (C_{3v}, X^1A_1)	ν_1 (cm^{-1})	1012[c]	979[c]	950[c]
	ν_2 (cm^{-1})	1634 (2)[b]	1628 (2)	1627 (2)
	ν_3 (cm^{-1})	3333	3339	3337
	ν_4 (cm^{-1})	3431 (2)	3442 (2)	3444
	A_e (cm^{-1})	6.3794	6.3483	6.196
	B_e (cm^{-1})	9.9225 (2)	9.9886 (2)	9.4443 (2)
	N–H (Å)	1.0129	1.0115	1.012
	∠XNH (degree)	112.6295	112.1051	112.15

[a]Taken from NIST Chemistry Webbook.[46]
[b]Value in the parenthesis presents the degeneracy.
[c]The umbrella vibration.

TABLE 2 Individual contributions (kJ mol^{-1}) of various terms calculated at 0 K using HEAT-456QP method (energies are given relative to the reactants, $H + NH_3$)

Term	$H_2 + NH_2$	TS
δE_{SCF}	–2.31	97.06
$\delta E_{CCSD(T)}$	27.72	–31.69
δE_{CCSDT}	–0.70	–1.07
$\delta E_{CCSDTQP}$	0.27	–0.04
δE_{Scalar}	–0.42	–0.35
δE_{ZPE}	–13.21	–6.72
	(–13.86)[a]	(–6.53)[a]
δE_{DBOC}	0.49	0.71
$\delta E_{Spin\text{-}orbit}$	0.00	0.00
Total energy	11.84	57.90
	(11.44 ± 0.15)[b]	

[a]Values in parentheses are obtained using harmonic zero-point vibrational energies.
[b]The value in parenthesis is derived from heats of formation at 0 K of H (216.034 kJ/mol), NH_3 (–38.562 ± 0.030 kJ/mol), H_2 (0 kJ/mol), and NH_2 (188.91 ± 0.12 kJ/mol), which are taken from ATcT.[40-43]

contribution, and brings the barrier close to the final value. Another important contribution is zero-point energy (ZPE), which cuts the barrier by 6.7 kJ/mol. The full triple, quadruple, and pentuple excitations that go beyond CCSD(T)) lower the barrier by an additional 1.1 kJ/mol. Contributions of the remaining terms are smaller, but essential for an accuracy of ca. 1 kJ/mol. Taking all individual contributions into account, the forward barrier height is obtained to be 57.9 ± 1 kJ/mol. To the best of our knowledge, HEAT-456QP is the highest level of theory that has been applied to the title reaction. Previous studies using various levels of theory reported the vibrationally adiabatic barrier height in the range of 55–65 kJ/mol.[19–26]

3.2 | Thermal rate coefficients

NH_3 has a well-known inversion ("umbrella") vibrational mode, for which the fundamental frequency is overestimated (with VPT2) by 29 cm^{-1} as compared to experiment (see Table 1). The following approximate procedure was used to treat this umbrella motion as an independent, one-dimensional hindered internal inversion (1DHI). First, we used the AE-CCSD(T)/aug-cc-pCVQZ level of theory to construct an inversion potential energy curve and an effective moment of inertia as a function of the inversion angle. Second, we solved a one-dimensional Schrödinger equation to obtain a set of eigenvalues of the 1DHI. Then, we directly counted the

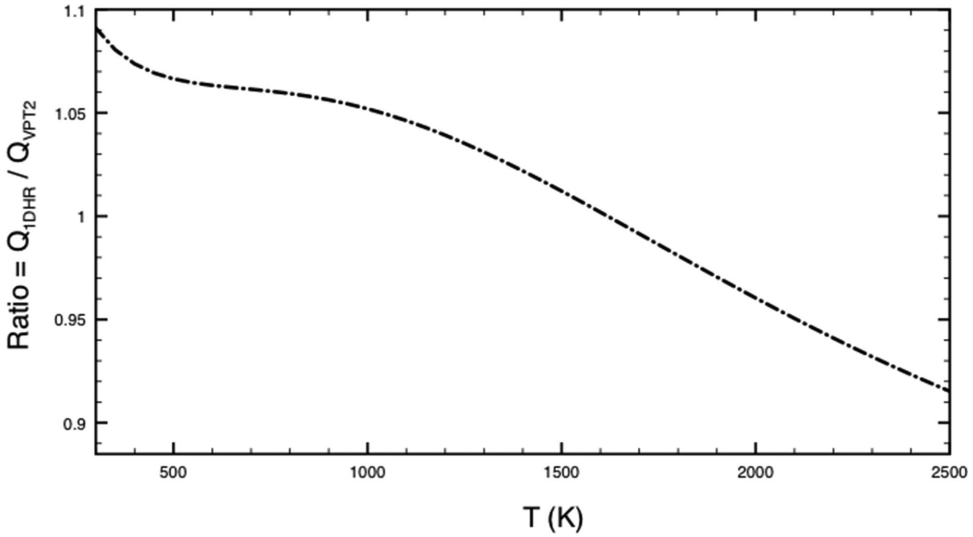

FIGURE 2 Ratio of 1DHI partition function over that of VPT2 calculated as a function of temperature for NH_3

density and sum of states as a function of internal energy. Finally, we convolved the 1DHI with the remaining vibrations to gain the quantum vibrational states for NH_3. It should be mentioned that the NH_3 inversion calculation used here gives a tunneling splitting of 1.3 cm^{-1}, in acceptable, and arguably good agreement with the experimental value of 0.79 cm^{-1}.[44] In addition, it yields an inversion ZPE of 507 cm^{-1}, which is 18 cm^{-1} lower than the VPT2 value of 525 cm^{-1}. This will impact the reaction enthalpy and the forward rate constants, but not the reverse ones, which are independent of the partition function of NH_3. A comparison of 1DHI with VPT2 approach is displayed in Figure 2. Inspection of Figure 2 shows a ratio of 1DHI partition function (including the change of 18 cm^{-1} in ZPE) over that of VPT2 as a function of temperature. As can be seen, the ratio decreases with temperature: it falls from ca. 1.09 at 300 K to ca. 0.92 at 2500 K. Overall, the 1DHI treatment changes the NH_3 vibrational partition function, but by no more than 10%.

For the reverse reaction ($H_2 + NH_2 \rightarrow H + NH_3$), Figure 3 shows the calculated rate constants increasing significantly with temperature. $k(T)$ rises by more than six orders of magnitudes between 300 and 2500 K: it is 1.5×10^{-18} cm^3 $molecule^{-1}$ s^{-1} at 300 K to 5.3×10^{-12} cm^3 $molecule^{-1}$ s^{-1} at 2500 K. The ab initio $k(T)$ values agree essentially quantitatively with all experimental results, which were measured by four different groups. To the best of our knowledge, this is the first study to achieve such accurate results for this reaction over an extensive temperature range.

To have a careful comparison of theory with experiment for the forward reaction ($H + NH_3 \rightarrow H_2 + NH_2$), we divide temperature into two regimes, namely, low to moderate T (450–1000 K) and moderate to high T (1000–2000 K). For T = 450–1000 K (see Figure 4A), our calculated rate constants agree well with the results of Ko et al.,[18] but marginally overestimate those of Hack et al.[13] and Marshall and Fontijn.[17] (According to Ko et al.,[18] the former results are more reliable than the latter two.) Note that both data sets were measured by the same group. For T = 1000–2000 K (see Figure 4B), again we slightly overestimate experiments by about 20%: our values are at the upper end of experimental results.

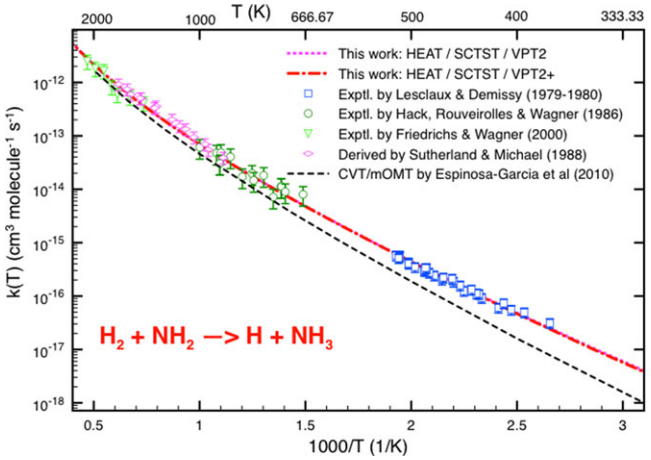

FIGURE 3 Thermal rate coefficients for the reaction $H_2 + NH_2 \rightarrow H + NH_3$ as a function of temperature calculated using both SCTST/VPT2 and SCTST/VPT2+ approaches. Experimental data are also included for comparison [Color figure can be viewed at wileyonlinelibrary.com]

The ab initio thermal rate constants from 300 to 2500K for both forward and reverse reactions can then be fit to a three parameter Arrhenius formula:

$k(T)_{H_2+NH_2} = AT^n e^{(B/T)}$, cm^3 $molecule^{-1}$ s^{-1} with A = exp(–44.8359), n = 2.58163, and B = −3290 (K).

$k(T)_{H+NH_3} = AT^n e^{(B/T)}$, cm^3 $molecule^{-1}$ s^{-1} with A = exp(–39.8793), n = 2.23036, and B = −5237 (K).

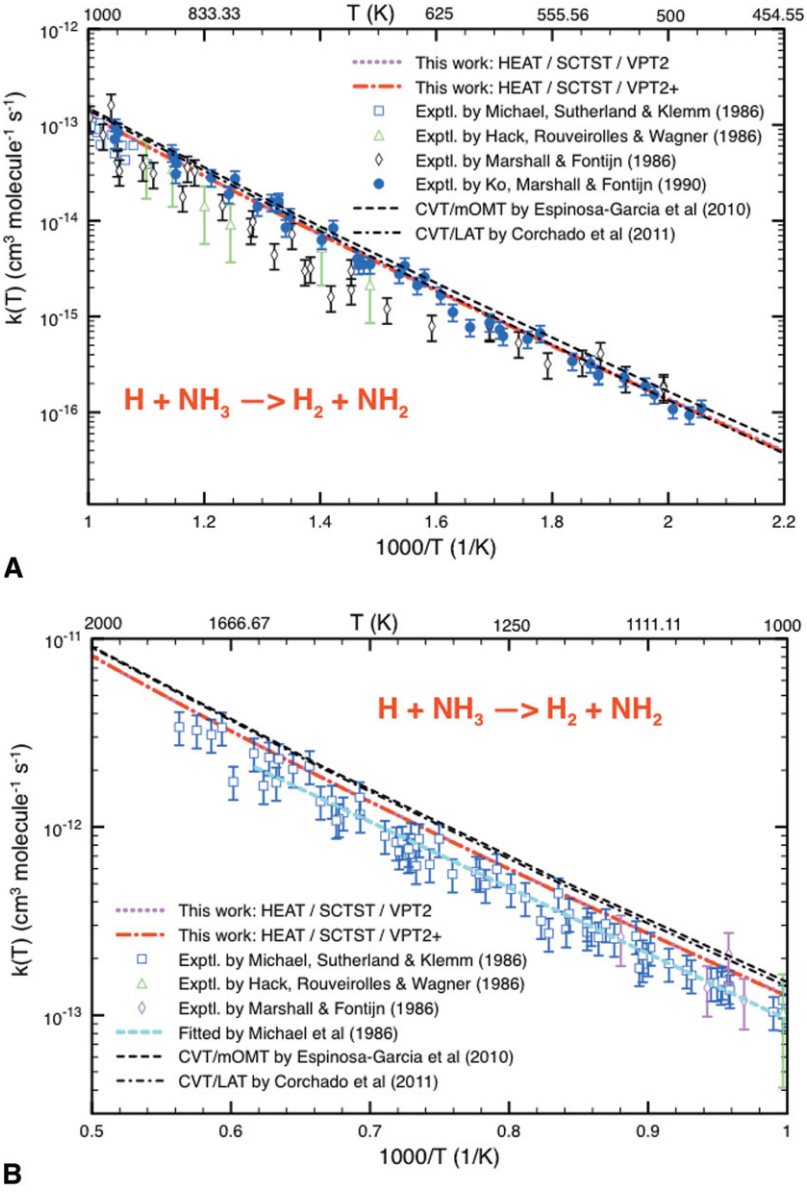

FIGURE 4 Thermal rate coefficients for the reaction $H + NH_3 \rightarrow H_2 + NH_2$ as a function of temperature calculated using both SCTST/VPT2 and SCTST/VPT2+ approaches: (A) below 1000 K and (B) above 1000 K. Experimental data are also included for comparison [Color figure can be viewed at wileyonlinelibrary.com]

Quantum mechanical tunneling effects play an important role for the title reaction, especially at low temperatures. Note that experimental results at $T \leq 298$ K are not available because the high barrier prevents reaction to proceed at an experimentally detectable rate at these conditions. Figure 5 shows the tunneling effects declining sharply with temperature: the enhancement is greater than 100 at 200 K, and then drops to ca. 7 at room temperature, and about 3 at 400 K. When temperature is more than 1400 K, the tunneling effects become unimportant.

It is of importance to compare the HEAT/SCTST rate constants with other theoretical calculations.[24,26] Tables 3 and 4 (also see Figures 3 and 4) display comparisons for the forward and reverse reactions of $H + NH_3 \rightleftharpoons H_2 + NH_2$, respectively. We chose to compare the SCTST results with two recent sets of theoretical $k(T)$ data calculated with the CVT/μOMT[24] and CVT/LAT[26] techniques of POLYRATE program,[45] based on the same PES-2009,[24] which was constructed using CCSD(T,fc)/cc-pVTZ.[20,24] Both of these sets of $k(T)$ are in close agreement with available experimental data. There are other CVT/LAT results reported earlier,[19,20] which are not included here for comparison because they were based on older and less accurate potential energy surfaces (PESs).[19,20] Inspection of Table 3 (also see Figure 4) shows that the SCTST results are in better agreement with those of Corchado et al.[26] than those of Garcia et al.[24] All three sets of theoretical results slightly overestimate experiment at the high-temperatures characteristic of combustion.[16] Overall, the agreement between two different techniques (HEAT/SCTST vs. CVT/μOMT) is excellent in the whole temperature range of 200–2000 K. The main differences largely arise from the choice of potential energy surface. Both kinetics approaches are nearly identical for this reaction so long as the same energetics are used.

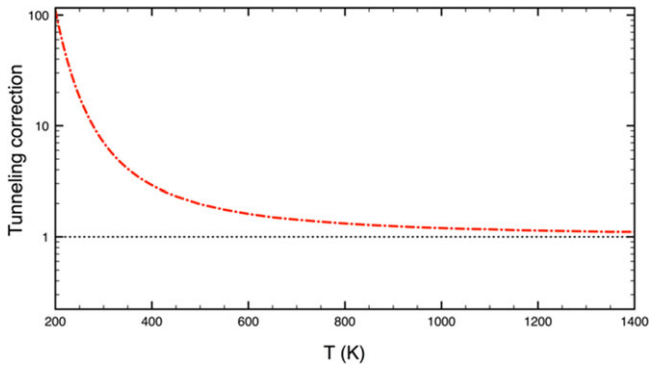

FIGURE 5 Multiple dimensional quantum mechanical tunneling correction as a function of temperature calculated using SCTST/VPT2+ approach [Color figure can be viewed at wileyonlinelibrary.com]

TABLE 3 A comparison of the calculated SCTST rate constants for $H + NH_3 \rightarrow H_2 + NH_2$ with CVT/μOMT and CVT/LAT results

T (K)	SCTST[a]	CVT/μOMT (2010)[b]	CVT/LAT (2011)[c]
200	7.58×10^{-24}	1.10×10^{-23}	5.34×10^{-24}
300	4.62×10^{-20}	5.78×10^{-20}	3.57×10^{-20}
400	6.05×10^{-18}	7.42×10^{-18}	5.47×10^{-18}
500	1.36×10^{-16}	1.65×10^{-16}	1.34×10^{-16}
600	1.19×10^{-15}	1.43×10^{-15}	1.23×10^{-15}
700	5.90×10^{-15}	7.09×10^{-15}	6.34×10^{-15}
1000	1.26×10^{-13}	1.50×10^{-13}	1.42×10^{-13}
1200	4.58×10^{-13}	5.35×10^{-13}	5.15×10^{-13}
1500	1.81×10^{-12}	2.08×10^{-12}	2.03×10^{-12}
2000	8.08×10^{-12}	9.09×10^{-12}	8.97×10^{-12}

[a]This work.
[b]The CVT/μOMT calculations were based on PES-2009.[24]
[c]The CVT/LAT calculations were based on PES-2009.[26]

TABLE 4 A comparison of the calculated SCTST rate constants for $H_2 + NH_2 \rightarrow H + NH_3$ with CVT/μOMT results

T (K)	SCTST (2017)[a]	CVT/μOMT (2010)[b]	Ratio = SCTST / CVT/μOMT
200	3.64×10^{-21}	4.16×10^{-22}	8.75
300	1.47×10^{-18}	3.39×10^{-19}	4.34
400	4.66×10^{-17}	1.60×10^{-17}	2.91
500	4.35×10^{-16}	1.88×10^{-16}	2.31
600	2.10×10^{-15}	1.05×10^{-15}	2.00
700	6.84×10^{-15}	3.80×10^{-15}	1.80
1000	6.97×10^{-14}	4.58×10^{-14}	1.52
1200	1.93×10^{-13}	1.34×10^{-13}	1.44
1500	5.95×10^{-13}	4.36×10^{-13}	1.36
2000	2.17×10^{-12}	1.69×10^{-12}	1.28

[a]This work.
[b]The calculations were based on PES-2009.[24]

However, there are significant differences between the calculated SCTST rate constants and CVT/μOMT results for the reverse reaction, $H_2 + NH_2 \rightarrow H + NH_3$. Table 4 displays the difference defined as a ratio of SCTST over CVT/μOMT rate constants. As seen in Table 4 (also see Figure 3), the difference declines with increasing temperature: it is a factor of ca. 8.8 at 200 K, 2.0 at 600 K, and reduces to ca. 1.3 at 2000 K. This problem is likely due to a possible energy error of about 3 kJ/mol for NH_2 in PES-2009[24] (e.g., $\Delta H_{f,\mathrm{ok}}$ (NH_2) = 185.8kJ/mol from PES-2009 as compared to ATcT's value[40–43] of 188.9 ± 0.1 kJ/mol). It should be noted here that the SCTST rate constants for this reverse reaction agree very well with all available experimental date (see Figure 3). This result implies that the equilibrium constants from the two PESs are different.

4 | CONCLUSIONS

The thermochemistry for the title reaction has been studied using the high-accuracy HEAT-456QP method, followed by chemical kinetic calculations using Miller's SCTST theory to obtain thermal rate coefficients at the high-pressure limit. The forward reaction pathway is endothermic by 11.8 ± 1 kJ/mol, which agrees very well with the ATcT value of 11.5 ± 0.2 kJ/mol.[40–43] The forward and reverse barrier heights (including ZPE corrections) were estimated to be 57.9 ± 1 and 46.1 ± 1 kJ/mol, respectively. The highly accurate thermochemistry in this work leads to a significant improvement of ab initio thermal rate constants, which now agree well with experimental results for the reverse reaction, for which all previously theoretical calculations were not successful. This certainly demonstrates the significant importance of accurate thermochemistry, even in kinetics calculations. Furthermore, thermal rate constants above 2500 K where experimental results are not available have been provided in Table S1 (see the Supporting Information Material) for kinetic modeling.

ACKNOWLEDGMENTS

This material is based on work supported by the U.S. Department of Energy, Office of Basic Energy Sciences under Award DE-FG02-07ER15884 and the U.S. Air Force Office of Scientific Research (No. FA9550-16-1-0117). Aspects of this work were also supported by the , under Grant CHE-1748821. We would also like to express our gratitude to two anonymous reviewers for their useful comments that improved the quality of this paper.

ORCID

Thanh Lam Nguyen
https://orcid.org/0000-0002-7794-9439

REFERENCES

1. Marban G, Vales-Solis T. Towards the hydrogen economy? *Int J Hydrogen Energ*. 2007;32:1625-1637.
2. Sherif SA, Barbir F, Veziroglu TN. Towards a hydrogen economy. *Electricity J*. 2005;18:62-76.
3. Balat M. Potential importance of hydrogen as a future solution to environmental and transportation problems. *Int J Hydrogen Energ*. 2008;33:4013-4029.
4. Miller JA, Bowman CT. Mechanism and modeling of nitrogen chemistry in combustion. *Prog Energ Combust*. 1989;15:287-338.
5. Klippenstein SJ, Harding LB, Glarborg P, Miller JA. The role of NNH in NO formation and control. *Combust Flame*. 2011;158:774-789.
6. Lyon RK. Method for the reduction of concentration of NO in combustion effluents using ammonia. US patent 3900554. 1973.
7. Zamfirescu C, Dincer I. Ammonia as a green fuel and hydrogen source for vehicular applications. *Fuel Process Technol*. 2009;90:729-737.
8. Zamfirescu C, Dincer I. Ammonia as a green fuel for transportation (pp. 507-515). In: Proceedings of the 2nd International Conference on Energy Sustainability. Vol. 1. August 10–14, 2008; Jacksonville, FL. Es2008-54328.
9. Zamfirescu C, Dincer I. Using ammonia as a sustainable fuel. *J Power Sources*. 2008;185:459-465.
10. Kang DW, Holbrook JH. Use of NH_3 fuel to achieve deep greenhouse gas reductions from US transportation. *Energy Rep*. 2015;1:164-168.
11. Nguyen TL, Stanton JF. High-level theoretical study of the reaction between hydroxyl and ammonia: accurate rate constants from 200 to 2500 K. *J Chem Phys*. 2017;147:15204-15207.
12. Demissy M, Lesclaux R. Kinetics of hydrogen abstraction by Nh2 radicals from alkanes in the gas-phase—a flash-photolysis laser resonance-absorption study. *J Am Chem Soc*. 1980;102:2897-2902.
13. Hack W, Kurzke H, Rouveirolles P, Wagner HG. Hydrogen abstraction reactions by $NH_2(X^2B_1)$-radicals from hydrocarbons in the gas-phase. *Ber Bunsen-Ges Phys Chem Chem Phys*. 1986;90:1210-1219.
14. Friedrichs G, Wagner HG. Direct measurements of the reaction $NH_2+H_2 \rightarrow NH_3+H$ at temperatures from 1360 to 2130 K. *Z Phys Chem*. 2000;214:1151-1160.
15. Sutherland JW, Michael JV. The kinetics and thermodynamics of the reaction $H + NH_3 <=> NH_2 + H_2$ by the flash-photolysis shock-tube technique—determination of the equilibrium-constant, the rate-constant for the back reaction, and the enthalpy of formation of the amidogen radical. *J Chem Phys*. 1988;88:830-834.
16. Michael JV, Sutherland JW, Klemm RB. Rate-constant for the reaction $H + NH_3$ over the temperature-range 750-1777-K. *J Phys Chem*. 1986;90:497-500.
17. Marshall P, Fontijn A. An Htp kinetics study of the reaction between ground-state H-Atoms and NH_3 from 500-K to 1140-K. *J Chem Phys*. 1986;85:2637-2643.
18. Ko T, Marshall P, Fontijn A. Rate coefficients for the $H + NH_3$ reaction over a wide temperature-range. *J Phys Chem*. 1990;94:1401-1404.
19. Garrett BC, Koszykowski ML, Melius CF, Page M. Theoretical calculations of the thermal rate constants for the gas-phase chemical-reactions $H + NH_3$ reversible $H_2 + NH_2$ and $D + ND_3$ reversible $D_2 + ND_2$. *J Phys Chem*. 1990;94:7096-7106.
20. Corchado JC, EspinosaGarcia J. Analytical potential energy surface for the $NH_3 + H <=> NH_2 + H_2$ reaction: application of variational transition-state theory and analysis of the equilibrium constants and kinetic isotope effects using curvilinear and rectilinear coordinates. *J Chem Phys*. 1997;106:4013-4021.
21. Moyano GE, Collins MA. Interpolated potential energy surface for abstraction and exchange reactions of $NH_3 + H$ and deuterated analogues. *Theor Chem Acc*. 2005;113:225-232.
22. Zhang XQ, Cui Q, Zhang JZH, Han KL. Quantum dynamics study of $H + NH_3 \rightarrow H_2 + NH_2$ reaction. *J Chem Phys*. 2007;126:234304.
23. Yang MH. Full dimensional time-dependent quantum dynamics study of the $H + NH_3 \rightarrow H_2 + NH_2$ reaction. *J Chem Phys*. 2008;129. https://doi.org/10.1063/1.2967854.
24. Espinosa-Garcia J, Corchado JC. Analytical potential energy surface and kinetics of the $NH_3 + H \rightarrow NH_2 + H_2$ hydrogen abstraction and the ammonia inversion reactions. *J Phys Chem A*. 2010;114:4455-4463.
25. Espinosa-Garcia J, Corchado JC. Quasi-classical trajectory calculations of the hydrogen abstraction reaction $H + NH_3$. *J Phys Chem A*. 2010;114:6194-6200.
26. Corchado JC, Espinosa-Garcia J, Yang MH. Kinetics and dynamics of the $NH_3 + H \rightarrow NH_2 + H_2$ reaction using transition state methods, quasi-classical trajectories, and quantum-mechanical scattering. *J Chem Phys*. 2011;135. https://doi.org/10.1063/1.3605242.
27. Song HW, Li J, Yang MH, Lu YP, Guo H. Nine-dimensional quantum dynamics study of the $H_2 + NH_2 \rightarrow H + NH_3$ reaction: a rigorous test of the sudden vector projection model. *Phys Chem Chem Phys*. 2014;16:17770-17776.
28. Li J, Guo H. A nine-dimensional global potential energy surface for $NH_4(X^2A_1)$ and kinetics studies on the $H + NH_3 \leftrightarrow H_2 + NH_2$ reaction. *Phys Chem Chem Phys*. 2014;16:6753-6763.
29. Song HW, Guo H. Effects of reactant rotational excitations on $H_2 + NH_2 \rightarrow H + NH_3$ reactivity. *J Chem Phys*. 2014;141. https://doi.org/10.1063/1.4904483.
30. Song HW, Yang MH, Guo H. Communication: equivalence between symmetric and antisymmetric stretching modes of NH_3 in promoting $H + NH_3 \rightarrow H_2 + NH_2$ reaction. *J Chem Phys*. 2016;145:131101.
31. Kalley M. MRCC, a quantum chemical program suite written by M. Kallay et. al. *J Chem Phys*. 2013;139:094105.
32. Stanton JF, Gauss J, Cheng L et al. CFOUR, a quantum chemical program package. For the current version, see http://wwwcfourde.
33. Nguyen TL, Stanton JF, Barker JR. A practical implementation of semi-classical transition state theory for polyatomics. *Chem Phys Lett*. 2010;499:9-15.
34. Nguyen TL, Stanton JF, Barker JR. Ab initio reaction rate constants computed using semiclassical transition-state theory: $HO+H_2 \rightarrow H_2O+H$ and isotopologues. *J Phys Chem A*. 2011;115:5118-5126.

35. Multiple-well BarkerJR. multiple-path unimolecular reaction systems. I. MultiWell computer program suite. *Int J Chem Kinet*. 2001;33:232-245.

36. Barker JR, Ortiz NF, Preses JM, et al. MultiWell-2016 software. 2016. http://clasp-research.engin.umich.edu/multiwell/.

37. Baer T, Hase WL. *Unimolecular Reaction Dynamics: Theory and Experiments*. New York: Oxford University Press; 1996.

38. Stanton JF. Semiclassical transition-state theory based on fourth-order vibrational perturbation theory: the symmetrical eckart barrier. *J Phys Chem Lett*. 2016;7:2708-2713.

39. Nguyen TL, Stanton JF. High-level theoretical study of the reaction between hydroxyl and ammonia: accurate rate constants from 200 to 2500 K. *J Chem Phys*. 2017;147. https://doi.org/10.1063/1.4986151.

40. Ruscic B. Uncertainty quantification in thermochemistry, benchmarking electronic structure computations, and active thermochemical tables. *Int J Quantum Chem*. 2014;114:1097-1101.

41. Ruscic B. Active thermochemical tables: sequential bond dissociation enthalpies of methane, ethane, and methanol and the related thermochemistry. *J Phys Chem A*. 2015;119:7810-7837.

42. Ruscic B, Boggs JE, Burcat A, et al. IUPAC critical evaluation of thermochemical properties of selected radicals. Part I. *J Phys Chem Ref Data*. 2005;34:573-656.

43. Ruscic B, Pinzon RE, von Laszewski G, et al. Active thermochemical tables: thermochemistry for the 21st century. *J Phys Conf Ser*. 2005;16:561-570.

44. Spirko V. Vibrational anharmonicity and the inversion potential function of NH_3. *J Mol Spectrosc*. 1983;101:30-47.

45. Truhlar DG, et al. POLYRATE 2015: computer program for the calculation of chemical reaction rates for polyatomics. 2015.

46. Linstrom PJ, Mallard WG, eds. *NIST Chemistry WebBook, NIST Standard Reference Database Number 69*. Gaithersburg MD: National Institute of Standards and Technology, Gaithersburg MD; 2018.

SUPPORTING INFORMATION

Additional supporting information may be found online in the Supporting Information section at the end of the article.

How to cite this article: Nguyen TL, Stanton JF. Ab initio thermal rate coefficients for H + NH_3 ⇌ H_2 + NH_2. *Int J Chem Kinet*. 2019;51:321–328. https://doi.org/10.1002/kin.21255